Conservation in High-field Quantum Transport

Mukunda P. Das¹ and Frederick Green^{2,*}

Department of Fundamental and Theoretical Physics, RSP,
 The Australian National University, Canberra, ACT 2601, Australia.
 School of Physics, The University of New South Wales, Sydney, NSW 2052, Australia.

We give a short overview of the role of microscopic conservation in charge transport at small scales, and at driving fields beyond the linear-response limit. As a practical example we recall the measurement and theory of interband coupling effects in a quantum point contact driven far from equilibrium.

I. INTRODUCTION

It is a given that any description of charge motion in an extended system must satisfy the continuity Equation [1]

$$\frac{\partial \rho}{\partial t} = -\nabla \cdot \mathbf{j} \tag{1}$$

tying the loss(gain) of local charge carrier *number* density $\rho(\mathbf{r},t)$, as a function of position and time, to the outflow(inflow) of the local carrier flux $\mathbf{j}(\mathbf{r},t)$. This dynamical identity is always accompanied by the static, or at least slowly time varying, Poisson Equation [1]

$$\nabla \cdot \mathbf{E} = -\nabla^2 \phi(\mathbf{r}, t) = \frac{e}{4\pi\varepsilon_0 \varepsilon} [\rho_0(\mathbf{r}) - \rho(\mathbf{r}, t; \phi)]$$
 (2)

where $\phi(\mathbf{r},t)$ is the local, conservative, electric potential and $\rho_0(\mathbf{r})$ is the compensating background ioncharge number density given at equilibrium, with ε the relative permittivity of the medium. Here we take ρ to describe the number density of mobile electrons.

Equations (1) and (2) define an electrical transport problem, be it classical or quantum [2], in which two exact conservation laws describe three coupled unknown functions. The practical issue is, naturally, to establish additional relations among them to close the computation. This is impossible to achieve exactly, including realistic situations such as quantum transport in conductors at the meso- and nanoscopic scales. A relevant model is the classic inverse Ohm's law, which posits $\mathbf{j} \equiv \sigma \cdot \mathbf{E}$ with σ the phenomenological conductivity tensor.

In this abridged review we first recall the elements underlying any microscopic description of circuit transport. In the second part we analyse a specific example: high-field current response in a quantum point contact (QPC), in which interband transitions are prominent. A minimum set of assumptions leads to a practicable transport solution that builds in conservation from the start. Their detailed outworking for the interband problem is in Reference [3]. A brief summary ends this paper.

II. PHYSICAL PICTURE

The fundamental premise underlying the entire study of transport is electrical neutrality of the whole system as is, of course, true [7] for every active electrical circuit. Over a system volume Ω this entails the *unconditional* constraint [1]

$$\int_{\Omega} d\mathbf{r} [\rho(\mathbf{r}, t; \phi) - \rho_0(\mathbf{r})] \equiv 0 = \iint_{\Sigma(\Omega)} \nabla \phi \cdot d\mathbf{A}$$
 (3)

^{*} frederickgreen@optusnet.com.au

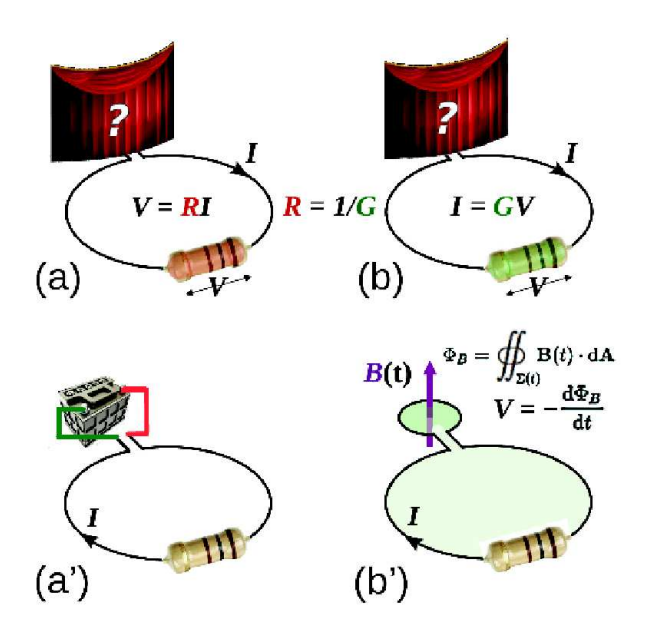


FIG. 1. Operational equivalence of a battery and a time-varying magnetic flux as nonconservative current sources for a generic closed circuit. As power supplies, both have lifetimes that are finite but sufficiently long relative to the time scale for measurement. With both sources notionally concealed, as in (a) and (b), there is no means to discriminate between the battery, (a'), and the changing flux, (b'), using only measurements on the active device. In either case the electromotive force cannot be described by a conservative potential. Such a potential is incapable of sustaining a constant circulating current. [4, 5].

The rightmost integral over the system surface $\Sigma(\Omega)$ expresses Gauss' theorem implying, from Equations (2) and (3), that any field line $\mathbf{E} = -\nabla \phi$ entering the neutral system must also leave it [6]. The potential generating such a field must be conservative and could not in itself sustain a net current across the bulk structure.

This begs the question of how to drive a current in steady state. The answer lies in the fact that a stable current (one possessing a period much longer than any measurement time) is physically possible only in a circuit geometry that is

- 1. multiply connected globally;
- 2. electrically neutral overall;
- 3. driven by a *nonconservative* internal field (the electromotive force, or EMF);
- 4. admits a mechanism dissipating absorbed power to the environment.

The paradigm of a nonconservative driver is a battery, but a time-varying magnetic flux threading the circuit loop is conceptually ideal as a driver (and as applied in power engineering), manifesting Faraday's law [4]. In Figure 1 we illustrate the operational equivalence of the two nonconservative ways of driving a conducting device.

In setting up a conserving transport description, the next step is to analyse the role of the macroscopic leads injecting and extracting the globally circulating current where it transits the active region. By their screening action, the strongly metallic leads re-establish total electrical neutrality within a very short distance (nanometres and less) from the regions where local accumulation and depletion of charge occurs at the interfaces with the lithographically defined device structure, which in the following will be a QPC.

Metallic screening at the boundaries means that the neutrality condition, Item 2 in the preceding list, applies more strictly to the QPC structure but not only that alone. It must be treated *together with* the immediate interfaces to the leads connecting it to the driving source. The interfaces are of one piece with

the nominal device structure. This means that a proper description will cover the device region up to and including the screening layers.

Charge neutrality does not depend on the EMF or the current. *The electrochemical potential in the bulk leads always remains fixed* [5], Passive mismatch of conservative electrochemical potentials is not the correct physical boundary condition for sustaining steady state [4].

A convenient way to conceive (not necessarily to implement) how to include the preceding physics into a theoretical description is to revise the continuity Equation for number density and current when driven by an external pump supplying current *I* to the active region; see also Figure 2. Simplifying to one dimension, Equation (1) is extended by introducing a point source and drain of particles in the right-hand side:

$$\frac{\partial \rho(x,t)}{\partial t} + \frac{\partial J(x,t)}{\partial x} = I(\delta(x+x_0) - \delta(x-x_0)). \tag{4}$$

In Equation (4) current is injected at location $-x_0$ standing in for the "upstream" boundary and reabsorbed at x_0 standing in for the "downstream" boundary. The operational length of the active region is then $L = 2x_0$. It is identifiable with the dominant mean free path (MFP) for scattering, since this is determined by collisions with the lead material at the interface regions. A general analysis of the electrodynamics of this scenario, from a fully microscopic viewpoint, was given by Sols [8] who analysed the boundary conditions for the quantum Kubo formula [5]. A formally different but equivalent microscopic description is found in Magnus and Schoenmaker [4].

To complete the formal framework one still needs two ingredients: (a) a functional connection between the local current distribution J and the local density ρ , and (b) a dissipative model of how the device material sheds the electrical energy pumped into the system's free energy by the power supply. Both of these can be accommodated by extending the form of the continuity Equation (1), and its generalisation Equation (4), to describe the carrier's momentum distribution as it evolves. This requires the kinetic quantum Boltzmann formalism, more fully elaborated in Ref. [9].

III. A NONEQUILIBRIUM PROBLEM

A. Setting the scene

In this Section we discuss the QPC transport experiment of de Picciotto *et al* [10, 11]. This experiment graphically reveals the need to go beyond single-carrier linear response to understand carrier kinetics at mesoscopic scales and below.

Our calculations to support such an understanding were done within the quantum Boltzmann protocol. In brief, the microscopic analogue to Equation (1) extends the object of interest to the distribution of electron number density $f_k(x,t)$ not only locally but in the space of available momentum states k, where the external field acts to promote them to a higher momentum:

$$\frac{\partial f_k(x,t)}{\partial t} + v_k \frac{\partial f_k(x,t)}{\partial x} + \frac{eE(x,t)}{\hbar} \frac{\partial f_k(x,t)}{\partial k} = -C_k[f](x,t). \tag{5}$$

here v_k is the group velocity in the conduction band of the electrons, and the field E is the sum of the external nonconservative EMF, which does *not* satisfy the Poisson Equation (2) and a reactive part that satisfies Equation (2) and so is conservative.

Crucially, the right-hand side of Equation (5) consists of an Ansatz encoding in *C* the collisional effects that tend to restore the distribution to its equilibrium Fermi-Dirac form as well as dissipating the energy gained from the driving field [4]. Since the local carrier-number density (leading factor of two is for spin) and its current are given by

$$\rho(x,t) = 2 \int \frac{dk}{2\pi} f_k(x,t) \text{ and } J(x,t) = 2 \int \frac{dk}{2\pi} v_k f_k(x,t),$$

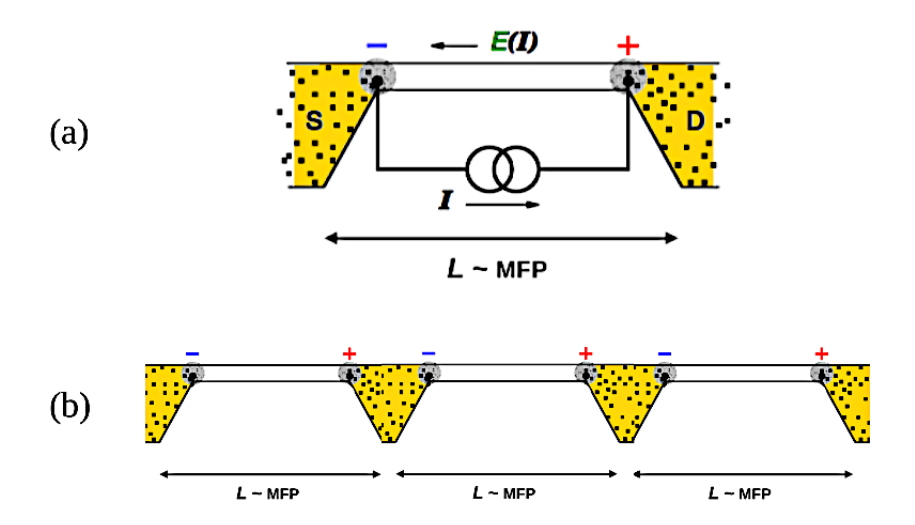


FIG. 2. (a) Schematic of a ballistic quantum point contact driven by an external current source and stabilised by bulk resistive metallic leads. Strong metallic screening at the interfaces enforces electrical neutrality in and charge uniformity over most of the device, independent of current I and EMF E(I). The scattering mean free paths, both elastic and dissipative, are bounded by the length scale including not only the impurity-free QPC geometry but also the adjacent regions of strong boundary scattering, where current enters and exits. The three structures together make up the complete physical device, whose operational length L delimits the longest mean free path. (b) An ensemble of identical such structures in series is conceptualised and described on the average. The current source and sink are now removed to the extremes of the ensemble.

conservation demands that, to recover Equation (1), integration on both sides of Equation (5) requires

$$\int \frac{dk}{2\pi} C_k[f](x,t) \equiv 0 \tag{6}$$

unconditionally [12]. Although the Boltzmann collision integral can be quite complicated, for practical use it may often be modelled more simply so long as Equation (6) is respected. In a one-dimensional channel, conductance is defined as the magnitude

$$G \equiv -e \frac{\partial J}{\partial V_{\rm sd}}$$

where V_{sd} is the source-to-drain EMF over the channel in the direction opposite to the flow J defined as positive (given electrons as the carriers of charge -e).

The important feature to keep in mind for the transport problem is that total charge neutrality for the QPC plus its screening boundaries, of operational length L as depicted in Figure 2, means that the total carrier number $N = \int_0^L dx \sum_k f_k(x,t)$ is fixed by the compensating background. It is independent of the current, This global constraint on the physics is as important as the identity (6) securing local conservation.

To introduce the experimental context we refer to the results shown in Figure 3, also due to dePicciotto and collaborators [10, 11]. In a quasi-one-dimensional (1D) quantum point contact, the restricted geometry results in a series of discrete subbands offset by energy gaps while, within each subband, carrier motion along the device remains free. At low driving currents the occupancies of the bands, and their contribution to device conductance, can be assumed to be uncoupled.

As the carrier density is increased via V_g , the capacitive gate voltage controlling the chemical potential, there is successive occupation of higher bands. Conductance increases in characteristic Landauer steps, each contribution from the carriers in the newly populated subband acting fully independently of its predecessors. Figure 3 illustrates this weak-field driven regime. Other than a slight nonideal shortfall in

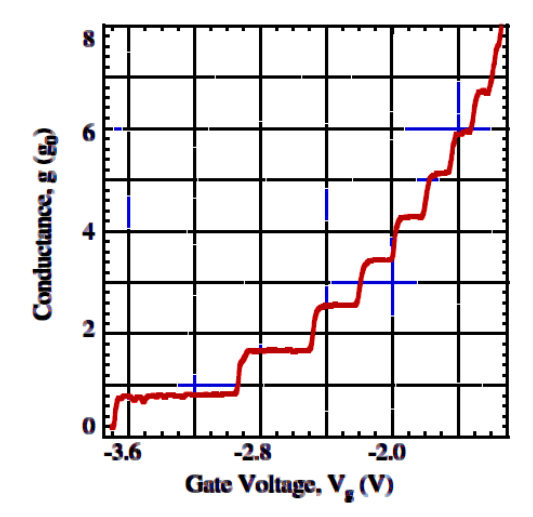


FIG. 3. Landauer conductance measured in a QPC [10, 11], adapted from dePicciotto *et al* [11]. Conductance is in units of the ideal step, $g_0 \approx 77.5 \mu S$. The experimental device was almost ideal, showing the low-field conductance rising in its characteristic steps, increasing discretely as each subband becomes newly occupied under the control of a gate voltage. The carriers in each band thus appear to contribute independently.

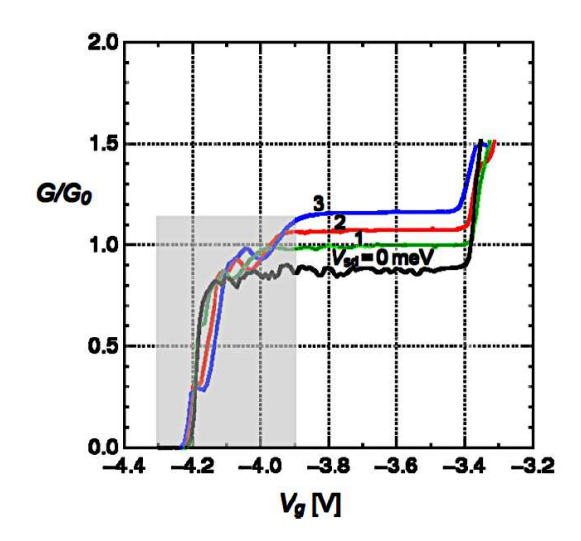


FIG. 4. QPC conductance G adapted from dePicciotto $et\ al\ [10,11]$ showing pronounced deviation of the Landauer steps from standard predictions. (Greyed-out band-threshold region covers the 0.7 anomaly [13], a quite different effect at onset, not of interest here.) Vertical scale for G is again in Landauer units. Nominally the gate voltage is set to restrict carrier density to the lowest occupied subband while $V_{\rm sd}$, the driving EMF along the channel, systematically increases. The QPC at low field ($V_{\rm sd}=0$) shows near-ideal behaviour, as in Figure 3. At progressively higher EMF, the step size of G increases and indeed exceeds the Landauer limit. This behaviour is not explicable by assuming carriers to move as single particles, within uncoupled bands. What is needed is a fully conserving kinetic description able to deal with dynamical interband cross-talk.

magnitude, the total device conductance increases stepwise as soon as the gate-controlled carrier density accesses each successively higher subband. There is no evidence of cross-talk or dynamical coupling among the discrete populations. As the kinetic-theoretical approach does [4], standard single-particle accounts also fit this and many other comparable measurements of QPC linear response.

B. Departure from linearity

Figure 4 [10, 11] presents a strikingly different scenario at fields substantially above the weak regime of Figure 3. In this experiment of dePicciotto and co-authors, the first interest was to explore the "0.7 anomaly", manifesting at the ground-state band threshold where *G* first starts to rise. The 0.7 phenomenon has been widely discussed, as evidenced not only by Refs. [10, 11] but also in the representative Refs. [13–15] and in the manifold citations therein.

In our research, here reviewed, we address the entirely distinct nonlinear response uncovered by the dePicciotto *et al* experiment. This novel type of QPC behaviour has not been mentioned, let alone analysed theoretically, anywhere in the 0.7 literature, other than in Refs. [10, 11] themselves.

At densities above the ground-state band threshold encompassing the 0.7 anomaly (greyed out in Figure 4 as it does not enter our discussion). the graph presents a series of traces for G, again as a function of V_g modulating the carrier density. The density regime is kept nominally within the lowest band, below the threshold for accessing the next higher band. The reported device had a working length of $2\mu m$; at a driving voltage $V_{sd} = 1V$ the internal field is $E = 5kVcm^{-1}$, well beyond the weak regime.

In this circumstance the conductance might have been expected to stay within the Landauer limit as seen at low field: $G \le G_0$. Evidently this is not so.

The Landauer limit is seen to be easily exceeded in Figure 4 as $V_{\rm sd}$ is raised, despite the carrier density's apparently remaining too low to access the next band and so induce an additional step in G. Moreover, the enhancement depends on the EMF and is manifestly nonlinear. Any linear-response account of the stepwise conductance would clearly be insufficient to explain its increasing nonlinear enhancement. It would be even less satisfactory to treat it as a collisionless single-particle transmission model.

A conserving approach based on the quantum Boltzmann Equation is able, with relatively simple assumptions, to reproduce the strongly nonequilibrium behaviour of Figure 4. The full formal description can be found in Ref. [3]. Here we sketch the concept behind it in terms of a form of Equation (5) in which two components, separated by a band gap, are coupled by collisional cross-talk in terms of interband scattering. This acts alongside the ever-present intraband scattering mechanisms.

The physical problem is one of active generation-recombination kinetics. There are two populations: one in the ground-state subband and (a no longer trivial) one in the next higher band. They couple through an interband scattering channel admitting particle exchange. Any carrier loss out of the low band must be reflected by an equal gain in the high band, and conversely.

Suppose f_{1k} is the low-band carrier number distribution and f_{2k} the higher one. The system of Equations to solve is

$$\frac{\partial f_{1k}}{\partial t} + v_k \frac{\partial f_{1k}}{\partial x} + \frac{eE}{\hbar} \frac{\partial f_{1k}}{\partial k} = -C_k[f_1] - C_{k;1 \to 2};$$

$$\frac{\partial f_{2k}}{\partial t} + v_k \frac{\partial f_{2k}}{\partial x} + \frac{eE}{\hbar} \frac{\partial f_{2k}}{\partial k} = -C_k[f_2] - C_{k;2 \to 1};$$
(7)

for simplicity we assume a uniform channel with uniform EMF field *E* [16].

As with Equation (6) the intraband collision terms $C_k[f_i]$, i = 1, 2 on the right-hand side of Equation (7) must each conserve separately *provided* the interband terms C ere absent and the bands stay blind to each other. To guarantee overall conservation, namely

$$2\int \frac{dk}{2\pi}(f_{k1} + f_{k2}) = \rho = \text{constant},$$

one has to arrange the physical model so

$$\sum_{i=1}^{2} \int \frac{dk}{2\pi} \left(C_k[f_i] + C_{k;i \to (3-i)} \right) \equiv 0.$$

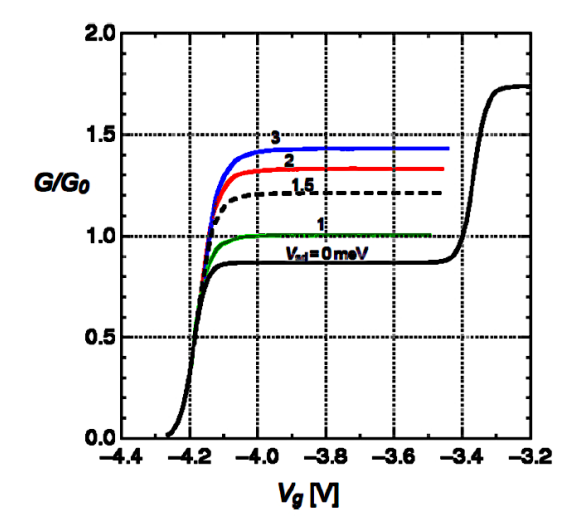


FIG. 5. QPC conductance corresponding the experimental case, Figure 4, computed within a conserving quantum Boltzmann model coupling two adjacent channel subbands [3]. At substantial driving fields, beyond the linear reguime, more carriers from the lower band gain sufficient energy to cross the energy gap and start to populate the higher band around its threshold, where G is most sensitive to small changes in population. The excited carriers enhance the net conductance, exceeding the Landauer limit, before collisional cross-coupling de-excites the promoted carriers to the lower band. In this approach it is natural for enhancement of G to be progressively greater as the driving voltage $V_{\rm sd}$ ramps up.

These constraints are not enough to close the coupled problem. An additional constitutive relation is needed and is provided by maximising the excess free energy of the nonequilibrium system [3].

The physical picture is that the free-motion acceleration by the EMF causes hot-electron energy to accumulate in the carriers until the dissipation rate from collisions matches the input power and this excess in free energy can rise no further, thus establishing steady state. The scenario is equivalent to the assumption of the balance of dynamical energy flows.

The inflow of external energy to the "reservoir" of hot-electron free energy, available for transfer to another medium, matches outflow to that medium, the ideal heat bath.

Figure 5 displays our calculation of nonlinear field enhancement of conductance in a QPC [3]. The strong similarity to experiment is clear. While our theory in its current form overemphasises nonlinear enhancement with source-drain voltage, there remains room to improve the quantitative accuracy. For instance, we have not implemented the energy-dependent emission of optical phonons in our inelastic relaxation rates. For an example of its role in hot-electron QPC noise, see Ref. [17]. In Figure 6 we show additional properties of our nonequilibrium coupled-band kinetics, from which two predictions follow: a common high-field saturation value for the enhancement, and the temperature dependence of its onset and growth rate with $V_{\rm sd}$.

The relative simplicity of assumptions for the Boltzmann-Drude collision terms C and C lead to a larger effect than seen in the experimental data of Figure 4. Refining the collision physics (for example, including optical phonon emission) would improve a quantitative match. Our priority has been to reproduce semi-quantitatively the salient aspects of the nonlinear transport effect as measured. The quantum kinetic model achieves this. and is open to refinement if new data were to emerge.

Allowing for transfer of highly excited carriers from the lower subband to the higher produces an
additional contribution to low-band conductance not otherwise envisaged in weak-field particle
transmission approaches.

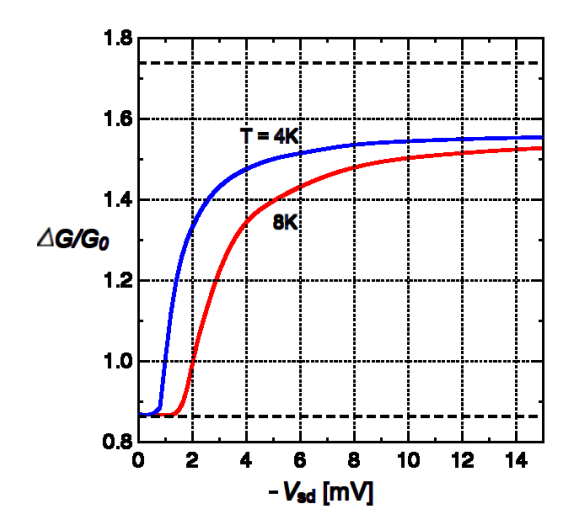


FIG. 6. Threshold and saturation behaviour of excess conductance ΔG versus source–drain voltage, at temperatures T=4K and 8K [3]. Lower dotted line is the base ground-state conductance step upper is for the second sub-band, both replicating band data from Ref. [10]. Two predictions for nonlinear QPC response are made: (1) the threshold driving field for onset of the enhancement scales approximately with T. (2) The saturation asymptote at high fields is independent of temperature and undershoots the contribution to G from the next higher band.

- Competition between excitation and dynamical relaxation of promoted carriers, assisted by stronger Pauli exclusion at higher densities, leads to a robustly flat set of conductance plateaux.
- While conductance enhancement increases with increasing driving field and readily exceeds the Landauer bound $G \le G_0$, its rate of increase tends to decline at larger EMF, pointing to saturation of the effect.

IV. SUMMARY

High-field conductance measurements of dePicciotto and co-workers [10, 11] were performed on exceedingly clean, almost ideal one-dimensional quantum point contacts. A major finding of their investigation was the pronounced nonlinearity of QPC conductance away from the more commonly explored linear response regime.

The experiment we have reviewed challenges received theories of quantised QPC conductance. It demands a more detailed kinetic theoretical analysis that pays due attention, first and last, to particle conservation at the level of its microscopic description. In this paper we have briefly recalled a viable quantum Boltzmann theory of nonlinear QPC conductance with reference to the above measurements.

The experimental results are already rather old, and have not been revisited in more detail since. Even in a field moving rapidly to sophisticated new types of excitations and their application to charge transport at small scales, the problems at high driving fields have not vanished. In fact they are likely to come into sharper focus than ever as the scale of active structures becomes shorter yet.

In our view, a renewed set of investigations in the regime away from linear response would stimulate more theoretical effort. That would provide a rational grounding for new design tools in the nanoelectronic panorama now emerging.

REFERENCES

- [1] Pines, D., and Nozières. P. The Theory of Quantum Liquids I; W. A. Benjamin: New York, NY, USA, 1966.
- [2] Frensley, W.R.; Einspruch, N.G. (Eds.) Heterostructures and Quantum Devices, a Volume of VLSI Electronics: Microstructure Science; Academic Press: San Diego, CA, USA, 1994.
- [3] Green, F.; Das, M.P. Anomalous conductance quantization in the inter-band gap of a one-dimensional channel. *J. Phys. Condens. Matter* **2018**, 30, 385304.
- [4] Magnus, W.; Schoenmaker, W. Quantum transport in Submicron Devices (Heidelberg: Springer-Verlag) 2002
- [5] Kamenev, A.; Kohn, W. Landauer conductance without two chemical potentials. Phys. Rev. B 2001, 62, 155304.
- [6] The possibility of field lines inside the medium looping back on themselves (that is, they are closed and multiply connected) is not excluded by Eq. (3) [4].
- [7] In a two- or one-dimensional context, the chemical potential and thus the charge for the system can be modulated, say capacitively, by an adjacent gate. In that case the compensating charge can be physically offset from the active structure; nevertheless bulk charge neutrality and the physics of boundary screening apply.
- [8] Sols, F. Phys. Rev. Lett. 1991, 67, 2874.
- [9] Green, F.; Das, M. P. Coulomb screening in mesoscopic noise. J. Phys.: Condens. Matter 2000, 12, 5251.
- [10] De Picciotto, R.; Pfeiffer, L.N.; Baldwin, K.W.; West, K.W. Nonlinear Response of a Clean One-Dimensional Wire *Phys. Rev. Lett.* **2004**, 92, 036805.
- [11] De Picciotto, R.; Baldwin, K.W.; Pfeiffer, L.N.; West, K.W. The 0.7 structure in cleaved edge overgrowth wires. *J. Phys. Condens. Matter* **2008**, 20, 164204.
- [12] On summing the left-hand side of Equation (5), the term carrying $\partial f_k/\partial k$ yields zero since the distribution f_k must go to zero at large momenta (or else the sum diverges and so would the density ρ).
- [13] Pepper, M.; Bird, J. The 0.7 feature and interactions in one-dimensional systems. *J. Phys.: Condens. Matter* **2008**, 20, 160301.
- [14] Micolich, A. P. What lurks below the last plateau: experimental studies of the $0.7 \times 2e^2/h$ conductance anomaly in one-dimensional systems. *J. Phys.: Condens. Matter* **2011**, 23, 443201.
- [15] Das, M. P. and Green, F. Conductance anomalies in quantum point contacts and 1D wires. *Adv. Nat. Sci.: Nanosci. Nanotechnol.* **2017** 8, 023001,
- [16] The source of the driving field E is external to the active 1D channel. Within the channel it is always so that $\partial E/\partial x = 0$. This is not the case for a driving field generated by mismatch of a continuous electrochemical potential (hence of local carrier density). On the other hand, as in Ref. [9] the role of screening from the macroscopic leads induces the carrier density in a typical channel to be uniform, in which case only the uniform, external, nonconservative EMF is the active driver.
- [17] Green, F.; Thakur, J. S; Das, M. P. Where is the Shot Noise of a Quantum Point Contact? *Phys. Rev. Lett.* **2004**, 92, 156804.